A correlation between hard gamma-ray sources and cosmic voids along the line of sight

A. Furniss, P. M. Sutter, J. R. Primack, A. Domínguez

HAL Id: insu-03644785
https://insu.hal.science/insu-03644785

A correlation between hard gamma-ray sources and cosmic voids along the line of sight

A. Furniss,[1][*] P. M. Sutter,[2,3,4] J. R. Primack[5] and A. Domínguez[6]

[1]*Department of Physics, Stanford University, Stanford, CA 94305, USA*
[2]*Sorbonne Universités, UPMC Univ Paris 06, UMR7095, Institut d'Astrophysique de Paris, F-75014 Paris, France*
[3]*CNRS, UMR7095, Institut d'Astrophysique de Paris, F-75014 Paris, France*
[4]*Center for Cosmology and AstroParticle Physics, Ohio State University, Columbus, OH 43210, USA*
[5]*Physics Department, University of California, Santa Cruz, CA 95064, USA*
[6]*Department of Physics and Astronomy, University of California, Riverside, CA 92521, USA*

ABSTRACT

We estimate the galaxy density along lines of sight to hard extragalactic gamma-ray sources by correlating source positions on the sky with a void catalogue based on the Sloan Digital Sky Survey (SDSS). Extragalactic gamma-ray sources that are detected at very high energy (VHE; $E > 100$ GeV) or have been highlighted as VHE-emitting candidates in the *Fermi* Large Area Telescope hard source catalogue (together referred to as 'VHE-like' sources) are distributed along underdense lines of sight at the 2.4σ level. There is also a less suggestive correlation for the *Fermi* hard source population (1.7σ). A correlation between 10 and 500 GeV flux and underdense fraction along the line of sight for VHE-like and *Fermi* hard sources is found at 2.4σ and 2.6σ, calculated from the Pearson correlation coefficients of $r = 0.57$ and 0.47, respectively. The preference for underdense sight lines is not displayed by gamma-ray emitting galaxies within the second *Fermi* catalogue, containing sources detected above 100 MeV, or the SDSS Data Release 7 quasar catalogue. We investigate whether this marginal correlation might be a result of lower extragalactic background light (EBL) photon density within the underdense regions and find that, even in the most extreme case of a entirely underdense sight line, the EBL photon density is only 2 per cent less than the nominal EBL density. Translating this into gamma-ray attenuation along the line of sight for a highly attenuated source with opacity $\tau(E, z) \sim 5$, we estimate that the attenuation of gamma-rays decreases no more than 10 per cent. This decrease, although non-negligible, is unable to account for the apparent hard source correlation with underdense lines of sight.

Key words: BL Lacertae objects: general – cosmology: miscellaneous – gamma-rays: galaxies.

1 INTRODUCTION

The flux from extragalactic very high energy (VHE; $E \geq 100$ GeV) gamma-ray sources is absorbed by extragalactic background light (EBL) photons via pair production in an energy- and distance-dependent manner (Nikishov [1962](); Gould & Shréder [1967]()). As a consequence of this absorption, the EBL produces an opacity $\tau(E, z)$ for VHE photons of observed energy E from a source located at redshift z. This opacity leads to an exponential flux attenuation $e^{-\tau(E, z)}$.

The EBL consists of all the evolving accumulated and reprocessed light from the ultraviolet (UV) to the far-infrared (IR) and is

difficult to measure directly due to strong foreground sources (e.g. Hauser & Dwek [2001]()). A selection of the currently available models of the EBL photon density includes a semi-analytical model (Gilmore et al. [2012]()), a model based on observations of galaxy spectral energy distribution fractions (Domínguez et al. [2011a]()), and a fitting, interpolating and multiwavelength backward evolution of cosmological survey data (Franceschini, Rodighiero & Vaccari [2008]()).

These EBL models estimate photon densities at or above the conservative lower limits derived from galaxy counts, and are each below the indirectly set upper limits based on the detection of extragalactic VHE photons from sources at $z \sim 0.1$–0.2 (e.g. Aharonian et al. [2006](); Meyer et al. [2012]()). More recent use of extragalactic gamma-ray sources for indirect studies of the EBL photon density have confirmed an EBL density not much above the observational

[*] E-mail: amy.furniss@gmail.com

$z \sim 0$ lower limits and confirmed the 'cosmic gamma-ray horizon', defined as $\tau(E, z) = 1$ (e.g. Ackermann et al. 2012; H.E.S.S. Collaboration 2013; Domínguez et al. 2013). However, even with a low EBL photon density, a number of distant blazars have recently been detected at energies that probe opacities between $\tau = 2$ and 5 (MAGIC Collaboration 2008; Becherini et al. 2012; Furniss et al. 2013; Archambault et al 2014). The most distant of the sources detected above 100 GeV thus far is PKS 1424+240, with the redshift lower limit of $z > 0.6$ (Furniss et al. 2013), which consistently displays a VHE flux of at least $(1.02 \pm 0.08) \times 10^{-7}$ photons cm^{-2} s^{-1} above 120 GeV (Archambault et al 2014). PKS 1424+240 has been detected at gamma-ray opacities of $\tau > 4.5$, with the specific value dependent on the EBL model used to estimate the opacity. When the unattenuated gamma-ray emission from this distant blazar is reconstructed using current EBL models, the spectrum shows a puzzling flattening or even upturn at the highest energies (Archambault et al 2014).

Various scenarios have been explored to account for the spectral shape of high energy emission of sources at high opacity values. These possibilities include lower EBL densities, as described in Furniss et al. (2013), the observation of secondary VHE emission resulting from extragalactic ultrahigh-energy cosmic rays (UHECR) interactions along the line of sight (LoS; e.g. Essey & Kusenko 2010), the existence of axion-like particles which couple to the high energy gamma-rays in the presence of a magnetic field (Domínguez, Sanchez-Conde & Prada 2011b; Horns & Meyer 2012; Harris & Chadwick 2014; Meyer, Montanino & Conrad 2014; Rubtsov & Troitsky 2014; Tavecchio, Roncadelli & Galanti 2014) and the possibility that VHE photons avoid pair production with the EBL through gravitational lensing (Barnacka, Böttcher & Sushch 2014). Each of the these scenarios, however, shares an important underlying assumption about the density of the EBL: they assume that, after accounting for the expected cosmological evolution of the photon field, at any redshift and wavelength the density of the EBL is homogeneous throughout intergalactic space.

We present preliminary examination of this assumption in this work. We perform a simple analysis to investigate a possible relationship between extragalactic VHE-like gamma-ray source directions and the density of matter along the LoS. In our analysis, VHE-like gamma-ray sources are sources that pass criteria on gamma-ray flux as measured by the *Fermi* Large Area Telescope (LAT; Atwood et al. 2009). See Section 3 for details on the VHE-like gamma-ray source list included in this study. We find an indication that VHE-like gamma-ray emitting galaxies (more specifically, blazars) might lie preferentially along underdense intergalactic lines of sight. We discuss the possibility that VHE-like gamma-ray sources are correlated with directions of lower than average EBL density, as this would result in a path of lower gamma-ray opacity for extragalactic gamma-rays.

2 METHOD

Since the galaxies that are sources of the EBL preferentially trace high-density regions within the cosmic web, the local light production should be proportional to the local matter density. Thus, regions with lower matter density, known as voids, should correlate with regions of lower local light production. We take the void sample from the Public Cosmic Void Catalog[1] (Sutter et al. 2012); specifically the *2014.11.04* release, as the tracer for regions of underdensity

within the Universe, and investigate the prevalence of voids along the lines of sight to blazars that lie within the Sloan Digital Sky Survey (SDSS) Data Release 7 (DR7) survey region.

The voids are identified within four volume-limited subsamples of the SDSS DR7 main sample (Strauss et al. 2002) from redshift $z = 0.05$ to 0.2 and a single volume-limited subsample from the SDSS luminous red galaxies (LRGs; Eisenstein et al. 2001) from $z = 0.16$ to 0.36. These correspond to the *dim1*, *dim2*, *bright1*, *bright2* and *lrgdim* samples, respectively. For this analysis we do not take higher redshift voids from SDSS Data Release 9 (DR9) because that survey has a more complicated geometry than the main sample, making the construction of fairly distributed random points difficult (see below). However, for two particularly distant sources, PKS 1424+240 and PG 1553+113, we utilize this higher redshift void catalogue from SDSS DR9. Since the DR9-derived void catalogue used in the analysis of these two sources is not used elsewhere, we do not include the results for these sources in the population investigations. When looking at different populations of sources, we utilize all voids within the catalogue, including those identified near the survey boundaries, since for our purposes we only wish to estimate the underdensity fraction along a given LoS, and do not need accurate distributions of void shapes.

Voids in the Public Catalog are identified with the VIDE toolkit (Sutter et al. 2015), which uses ZOBOV (Neyrinck 2008) to perform a Voronoi tessellation to estimate the density field from the galaxy population and a watershed transform to merge regional basins into voids. The Voronoi tessellation is a segmentation of the volume by a set of polyhedra such that the polyhedra describe the local volumes of each galaxy. Hence these polyhedra (called Voronoi cells) can be used to estimate the density field of the galaxy population. VIDE ensures that identified voids do not extend outside the survey mask. In the watershed picture, a void is a non-spherical aggregation of Voronoi volumes (Platen, van de Wygaert & Jones 2007) and can in principle have any mean or minimum density. However, they do represent basins in the density field (Sutter et al. 2013), and thus we can use them to estimate the underdense fraction. While the cores of watershed-based voids have densities below $0.2\rho_{\mathrm{mean}}$, at the effective radius (see below), the spherically averaged density inside a void is roughly $0.8\rho_{\mathrm{mean}}$ (Sutter et al. 2012).

VIDE provides two essential definitions used throughout this work. The first is the effective radius of a void:

$$R_{\mathrm{eff}} \equiv \left(\frac{3}{4\pi} V \right)^{1/3}, \tag{1}$$

where V is the total volume of all the Voronoi cells that make up the void. The second is the *macrocentre*, or volume-weighted centre of all the Voronoi cells in the void:

$$X_v = \frac{1}{\sum_i V_i} \sum_i \boldsymbol{x}_i V_i, \tag{2}$$

where $\boldsymbol{x}_i$ and V_i are the positions and Voronoi volumes of each galaxy i, respectively.

The voids have a typical size (median) of $R_{\mathrm{eff}} \approx 20 \, h^{-1}$ Mpc, but range anywhere from 5 to $60 \, h^{-1}$ Mpc. For simplicity, we approximate the voids as spheres with $R = R_{\mathrm{eff}}$ and place them on the sky according to their macrocentres.

We parametrize the relative underdensity along the LoS to an extragalactic source through the 'voidiness' (V_{LoS}), which is the fraction of the comoving LoS distance through underdense regions

---

[1] http://www.cosmicvoids.net

Table 1. Source catalogues included in this study. See text for a more detailed description of each.

Catalogue	Reference	Number of sources[a]	Energy range
SDSS quasars	Schneider et al. (2010)	3901	Optical
2LAC	Ackermann et al. (2011)	51	100 MeV–100 GeV
1FHL	Ackermann et al. (2013)	28	>10 GeV
VHE-like	Ackermann et al. (2013)	19	>50 GeV[b]
Randomly generated	–	1×10^5	–

[a]Sources within SDSS DR7 survey region and having a redshift of $0.05 < z < 0.36$.

[b]Which have gamma-ray properties that pass the following criteria, predetermined within the 1FHL catalogue: (1) the flux above 50 GeV being greater than 1×10^{-11} photons cm^{-2} s^{-1}; (2) a spectral index Γ above 10 GeV of less than 3; (3) a measure of the source significance above 30 and 100 GeV $(\text{Sig}_{30} = \sqrt{\text{TS}_{30\text{-}100} + \text{TS}_{100\text{-}500}} > 3)$. See text for details.

of space (voids) as compared to the total LoS distance to a source. More specifically,

$$V_{\text{LoS}} = \frac{\sum D_{\text{void},i}}{D_{\text{total}}}, \tag{3}$$

where $D_{\text{void},i}$ is the comoving intersectional LoS distance through a single void i and D_{total} is the total comoving LoS distance to the source. A higher V_{LoS} corresponds to a LoS that intersects a greater fraction of voids, while a low V_{LoS} corresponds to a lower fraction of underdense intersection.

As a cross-check, we calculate D_{void} in two independent ways. The first is a more simplistic method that associates a source to a void if the radial distance between the source and the void is less than the void radius after projecting the source and the void on the sky. For voids with $z_{\text{void}} < z_{\text{source}}$, the $D_{\text{void},i}$ is estimated as $(4/3)R_{\text{eff}}$, which is the average length of random intersections through a spherical region of radius R_{eff} (Coleman 1989). We also calculated D_{void} using an alternative approach that discretized each line connecting the observer to the source into many ($\sim$1000) points. We then obtained V_{LoS} by counting the fraction of line segments that lay within R_{eff} of each void macrocentre. This more careful and more expensive calculation resulted in no significant differences. Here, we present the detailed results utilizing the former method.

3 SOURCE CATALOGUES

The analysis is completed for multiple catalogues of both gamma-ray emitting and non-emitting extragalactic sources. The catalogues included are summarized in Table 1. Our studies are restricted to the catalogue sources that are within the SDSS DR7 survey region and have a spectroscopically determined redshift of $0.05 < z < 0.36$. The source populations are compared to a random set of points uniformly distributed throughout the SDSS DR7 survey region. We also investigate the lines of sight for the sources within the SDSS quasar catalogue, which includes confirmed quasars from the SDSS DR7 (Schneider et al. 2010), as well as the second *Fermi* catalogue of active galactic nuclei (2LAC; Ackermann et al. 2011).

The catalogue of sources detected by the *Fermi* LAT above 10 GeV is referred to as the 1FHL catalogue (Ackermann et al. 2013). This catalogue is built using analysis which focuses on energies above 10 GeV. The number of 1FHL sources that have associations with VHE emitters detected by Imaging Atmospheric Cherenkov Telescopes (IATCs) is 84. This is a significant portion of the 123 known VHE emitters at the time of 1FHL publication. Notably, the majority of the sources with VHE associations not included in the 1FHL catalogue are spatially extended Galactic VHE sources. There are only five point-like VHE sources that are not in 1FHL catalogue: the starburst galaxies NGC 253

and M82 and the blazars 1ES 0414+009, 1ES 0229+200 and 1ES 1312−423. None of the aforementioned blazars falls within the SDSS DR7 survey region and therefore are not included in this study despite their VHE detection.

We explicitly choose not to use the VHE catalogue[2] directly in this study. The ground-based detections of VHE-emitting sources by IACTs are typically obtained through pointed observations triggered by elevated emission of a source, and therefore likely result in a high-state biased population. This bias could be misleading when looking at correlations between V_{LoS} and the gamma-ray flux from a source, as done in Section 4. For this reason, we also remove 1ES 0806+524 from this study, the *only* 1FHL source within the SDSS DR7 survey region noted to display significant variability above 10 GeV.

We calculate the V_{LoS} for all 1FHL sources in the SDSS DR7 survey region with $0.05 < z < 0.36$. We also pay special attention to sources that pass a subset of cuts on gamma-ray emission properties to highlight candidate VHE sources that had not yet been detected by ground-based IACTs. The cuts were defined within the 1FHL catalogue. The 1FHL sources are flagged as good VHE candidates based on three properties: (1) the flux above 50 GeV being greater than 1×10^{-11} photons cm^{-2} s^{-1}; (2) a spectral index Γ_{10} above 10 GeV of less than 3; (3) a measure of the source significance above 30 and 100 GeV $(\text{Sig}_{30} = \sqrt{\text{TS}_{30\text{-}100} + \text{TS}_{100\text{-}500}} > 3)$, where $\text{TS}_{30\text{–}100}$ and $\text{TS}_{100\text{–}500}$ are the test statistic (TS) values[3] from the 30–100 and 100–500 GeV energy bands.

As this VHE candidacy criterion selects all VHE-detected sources at $0.05 < z < 0.36$, we refer to this population as 'VHE-like' for the remainder of this work. A full list of all 1FHL sources within the SDSS DR7 survey region and that have spectroscopic redshift $0.05 < z < 0.36$ is provided in Table 2. Note that VHE-like source list includes both VHE-detected and VHE-candidate sources, denoted with a Y and C in column 5 of Table 2, respectively. Additionally, the 1FHL integral gamma-ray flux (F_{10}) and index (Γ_{10}) are also included.

4 RESULTS

The restrictions on the spatial location and cosmological distance limits the sources from each catalogue included in this study. The number of sources within these restrictions is summarized in Table 1 for each catalogue. For the 1FHL sources, Table 2 includes the V_{LoS} of each source, as well as information on which sources reside

---

[2] http://tevcat.uchicago.edu/

[3] See Mattox et al. (1996) for TS definition, a statistic used in *Fermi* LAT source analysis.

Table 2. 1FHL sources $0.05 < z < 0.36$ within the SDSS DR7 footprint, ordered by increasing V_{LoS}. Sources marked with 'Y' are VHE detected, sources marked with 'C' are VHE candidates and sources marked with 'N' are not VHE detected and do not pass the VHE-candidate cuts summarized in Section 3.

| Name	RA	Dec.	Redshift	VHE detection?	$F_{10} \times 10^{-11}$ $(\mathrm{cm}^{-2}\,\mathrm{s}^{-1})$	Γ_{10}	V_{LoS}	In void?
RX J1136.5+6737	173.939	67.612	0.13	Y	11.7 ± 3.3	1.98 ± 0.34	0.00	No
PKS 0829+046	128.000	4.484	0.17	N	11.9 ± 4.1	2.61 ± 0.57	0.00	No
RX J0847.1+1133	131.773	11.544	0.2	Y	9.6 ± 3.6	1.45 ± 0.39	0.00	No
RGB J2313+147	348.514	14.769	0.16	C	10.6 ± 3.8	1.77 ± 0.39	0.00	No
H1426+428	217.158	42.659	0.13	Y	21.2 ± 4.8	2.01 ± 0.29	0.00	No
PG 1437+398	219.835	39.555	0.35	N	5.9 ± 2.6	1.79 ± 0.49	0.02	No
PKS 1509+022	228.064	2.074	0.22	N	11.1 ± 4.1	2.98 ± 0.70	0.03	No
1RXS J115404.9−001008	178.525	−0.169	0.25	N	11.6 ± 4.1	2.21 ± 0.54	0.03	No
PMN J1256−1146	194.110	−11.77	0.06	C	11.9 ± 4.1	2.07 ± 0.44	0.05	No
1ES 1440+122	220.737	11.982	0.16	Y	7.8 ± 3.5	1.77 ± 0.47	0.20	Yes
1ES 0806+534[a]	122.461	52.294	0.14	Y	45.3 ± 6.7	2.14 ± 0.20	0.21	No
SBS 1200+608	180.807	60.471	0.07	C	5.3 ± 2.4	1.63 ± 0.49	0.25	No
RBS 0958	169.305	20.227	0.14	C	23.4 ± 5.4	1.94 ± 0.28	0.29	No
OJ 287	133.712	20.079	0.31	N	11.1 ± 3.9	2.68 ± 0.59	0.30	Yes
MS 1458.8+2249	225.275	22.639	0.23	N	17.2 ± 4.7	1.89 ± 0.32	0.30	No
ON 246	187.586	25.377	0.14	N	7.3 ± 3.1	3.29 ± 0.95	0.41	No
RX J1136.8+2551	174.267	25.893	0.16	C	7.3 ± 3.1	1.62 ± 0.44	0.49	Yes
MS 1221.8+2452	186.146	24.628	0.22	C	7.7 ± 3.1	1.26 ± 0.38	0.49	No
BZB J1417+2543	214.659	25.658	0.24	N	8.4 ± 3.4	2.62 ± 0.70	0.53	No
H1013+498	153.773	49.427	0.21	Y	78.7 ± 8.9	2.28 ± 0.16	0.54	Yes
RX J1100.3+4019	165.165	40.315	0.23	C	11.2 ± 3.8	2.23 ± 0.45	0.60	Yes
B2 1229+29	187.970	28.824	0.24	C	28.3 ± 5.9	2.47 ± 0.33	0.61	No
W Comae	185.402	28.247	0.1	Y	34.1 ± 6.4	2.18 ± 0.26	0.62	No
GB6 J1053+4930	163.403	49.521	0.14	C	7.7 ± 2.9	1.49 ± 0.37	0.62	No
TXS 1055+567	164.666	56.459	0.14	C	44.4 ± 6.5	2.02 ± 0.19	0.72	No
PG 1218+304	185.337	30.194	0.18	Y	57.2 ± 8.6	1.90 ± 0.18	0.78	No
B2 1147+24	177.711	24.320	0.2	N	7.2 ± 3.0	4.14 ± 1.28	0.83	Yes
1ES 1215+303	184.460	30.104	0.13	Y	51.6 ± 8.2	2.11 ± 0.21	0.83	Yes

[a]Removed from analysis as the single source in this study showing a variability index of 2, as noted in the 1FHL catalogue (Ackermann et al. 2013).

within a void. The sources from each catalogue are distributed similarly within the survey volume. More specifically, seven of the 28 1FHL sources reside within a void (25 per cent of 1FHL sources). Five of the 19 VHE-like sources are within voids (26 per cent). These fractions are consistent with the fraction of SDSS quasars that are found within a void (710 of 3901; 18 per cent). Similarly, the randomly distributed points have a 21 per cent in-void fraction.

Fig. 1 shows the normalized histograms of source V_{LoS} for the various catalogues. The V_{LoS} of the randomly generated sample of points peaks at low $V_{\mathrm{LoS}} < 0.2$, with the fraction of sources decreasing with greater V_{LoS}. Less than 1 per cent of the randomly distributed sources show $V_{\mathrm{LoS}} > 0.8$. The slight peak in the distribution of randomly generated sample points near $V_{\mathrm{LoS}} \sim 0.5$ is due to the underlying redshift distribution of the voids.

The SDSS quasars follow a pattern in the V_{LoS} distribution that is similar to the randomly distributed sample of points. The SDSS quasars, however, have a higher fraction of sources at low $V_{\mathrm{LoS}} < 0.2$ (55 per cent as compared to 42 per cent for randomly distributed sources). The number of SDSS quasars with $V_{\mathrm{LoS}} > 0.8$ is less than 1 per cent, again similar to the randomly distributed sample of points.

The V_{LoS} distributions of the 2LAC sources are similar to the randomly generated and SDSS quasars, although not as steeply peaked at low V_{LoS}. However, the 1FHL and VHE-like distributions of V_{LoS} are dissimilar to the random distribution in shape: these distributions tend to prefer higher values of V_{LoS}. For a more rigorous statistical test of independence between each V_{LoS} distribution,
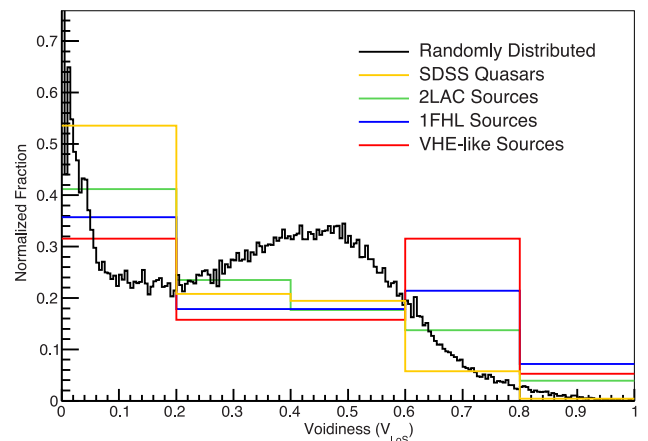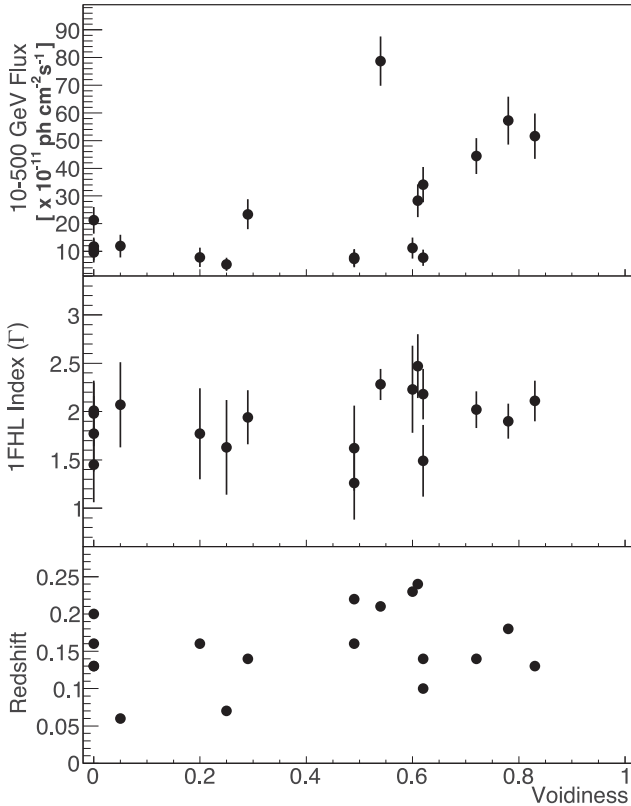

Figure 1. Normalized histograms of 'voidiness' V_{LoS} (equation 3) for the catalogue populations (randomly generated: black; SDSS: yellow; 2LAC: green; 1FHL: blue; VHE-like: red). See Table 2 for KS test results.

we performed a Kolmogorov–Smirnov (KS) test, with the P-values and the corresponding significances summarized in Table 3. The VHE-like V_{LoS} distribution is marginally different than the distribution from the randomly distributed points: we can reject the null hypothesis at the 2.1σ level that these two samples are drawn from the same distribution. A similar significance holds compared to the SDSS quasars (2.4σ), while the 2LAC V_{LoS} distribution is

Table 3. Cross-correlation of voidiness for different source populations. KS test results include P-values as well as the corresponding significance.

	Random	SDSS	2LAC	1FHL
Random	1			
SDSS	1.6×10^{-35} (12.5σ)	1		
2LAC	0.63 (0.5σ)	0.4 (0.9σ)	1	
1FHL	0.13 (1.5σ)	6.2×10^{-2} (1.7σ)	0.83 (0.2σ)	1
VHE-like	3.9×10^{-2} (2.1σ)	1.8×10^{-2} (2.4σ)	0.39 (0.9σ)	0.999 (0.0σ)

Figure 2. V_{LoS} of the VHE-like sources as compared to the source hard gamma-ray flux F_{10} (top panel), the 1FHL index Γ_{10} (middle panel) and the source redshift (bottom panel).

consistent with both the random and SDSS distributions (at 0.5σ and 0.9σ, respectively). Less significant is the 1FHL V_{LoS} distribution independence from the random and SDSS distributions at 1.5σ and 1.7σ, respectively. It is not entirely surprising that there is no significant independence among the 2LAC, 1FHL and VHE-like distributions of V_{LoS} as there is significant overlap among these source lists.

The results of the KS tests, and more specifically, the independence of the V_{LoS} distributions for the VHE-like sources as compared to the randomly generated and SDSS V_{LoS} distributions, suggest that the distribution of the VHE-like gamma-ray sources may be related to the intervening matter density in a different way than the quasar distribution. We investigate whether the level of intervening material might be related to the detection of gamma-ray emission by looking for a correlation between the V_{LoS} and the gamma-ray flux above 10 GeV for the VHE-like sources, as shown in Fig. 2. A constant fit to the V_{LoS} versus F_{10} results in a χ^2 of 175 for 17 degrees of freedom, not providing a good representation, especially at the higher values of V_{LoS}.

The Pearson correlation coefficient (r) is a measure of the linear dependence between two variables. This statistical test shows an indication of correlation between V_{LoS} and the gamma-ray flux of the VHE-like sources above 10 GeV (F_{10}), while there is no evidence of a correlation between V_{LoS} and the source index Γ_{10} or redshift. More specifically, for the VHE-like sources r is 0.57 (2.4σ; 18 sources) for V_{LoS} versus F_{10}, 0.25 for V_{LoS} versus Γ_{10} and 0.2 for V_{LoS} versus redshift. For the 1FHL sources, there is also a marginal correlation between V_{LoS} and the source hard gamma-ray flux with a r value of 0.47 ($\sim 2.6\sigma$; 28 sources) when testing V_{LoS} versus F_{10}. The r value is only 0.2 when testing V_{LoS} versus Γ_{10}, and 0.0 when testing V_{LoS} versus redshift.

5 DISCUSSION

We present a preliminary investigation on the assumption that the EBL density is homogeneous. The indication that the projected location of extragalactic VHE-like sources is related to the intervening matter density aligns with the hypothesis that the EBL density is spatially inhomogeneous. Only the local contribution to the spatial density of EBL photons is expected to scale with the local number density of galaxies. This local contribution cannot be more than a small fraction of the total EBL, which mostly arises from distant sources. Each spherical shell around any point contributes approximately equally, since the r^{-2} fall-off of light is compensated by the r^2 increase in area; contributions from higher redshifts suffer from redshifting and dilution by the expansion of the universe. However, since the opacity is an integral along the entire LoS from a blazar, even a relatively small decrease in the local EBL density could have a cumulative effect sufficient to affect the total gamma-ray opacity significantly. This could remove the motivation to exploit scenarios that utilize secondary VHE emission produced along the LoS or hypothetical axion-like particles to describe the VHE spectral flattening of the intrinsic emission from distant VHE gamma-ray sources such as PKS 1424+240.

Motivated by the apparent correlation between VHE-like sources and the fraction of void space along the LoS, we use another component of the public void catalogue that extends to $z = 0.65$ (derived from the SDSS DR9 survey region) to investigate the V_{LoS} of the exceptionally distant VHE-detected sources PKS 1424+240 at $z > 0.6035$ and PG 1553+113 at $z > 0.43$. Both of these sources are within the SDSS DR7 and DR9 survey regions and are noted in the 1FHL catalogue as VHE-detected sources that display VHE-like gamma-ray flux qualities. Under the assumption that the sources are located at the redshift lower limits, we find the V_{LoS} for PKS 1424+240 and PG 1553+113 are 0.74 and 0.63, respectively. Because of the use of an additional void catalogue in the calculation of the V_{LoS} for these sources, we do not include these sources in the statistical tests performed on the full catalogues, but the relatively high values of V_{LoS} for each are consistent with our findings from the DR7 survey region alone.
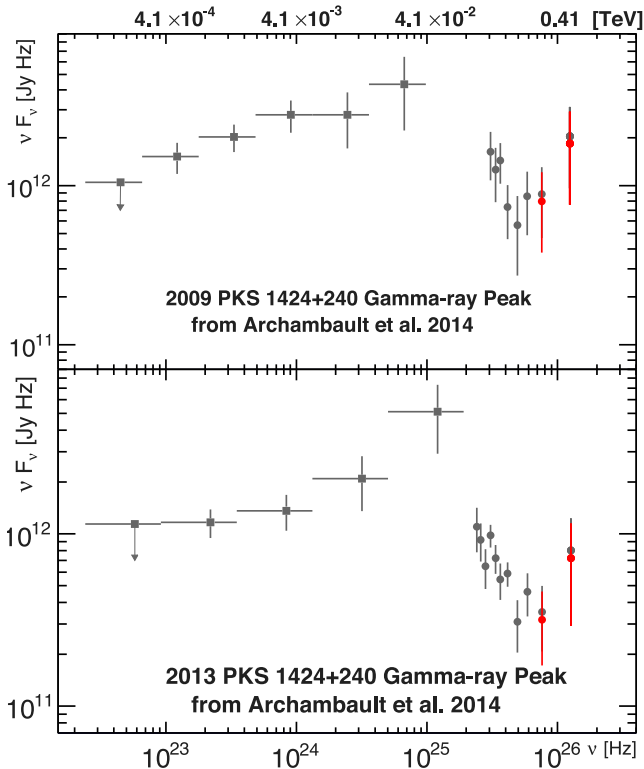
Figure 3. The absorption-corrected gamma-ray peak of PKS 1424+240 from Archambault et al ([2014](#)) as corrected by the Gilmore et al. ([2012](#)) model (black points) and for the $\tau\, p$ lower absorption resulting from the $p = 2$ per cent lower EBL density (red points). Below 300 GeV, the black and red points are indistinguishable and therefore are left as black.

We estimate the change in opacity for extragalactic VHE photons travelling along lines of sight that intersect many voids through the investigation of an extreme case. With the simplifying assumption that a gamma-ray emitting source lies along a sightline surrounded by a 50 h^{-1} Mpc radius tunnel that is devoid of galaxies, we find that the EBL density within this tunnel is only about 2 per cent lower than the nominal EBL density, as predicted independently by both the Gilmore et al. ([2012](#)) and Domínguez et al. ([2011a](#)) models. The effect on the attenuation of gamma-rays will be slightly larger than 2 per cent since the attenuation for gamma-rays is derived from the exponent τ. More specifically, the attenuation decreases by approximately $\tau\, p$, where p represents the percentage decrease in EBL density. For example, for an opacity of $\tau \sim 5$, as probed through the detection of PKS 1424+240 at the highest gamma-ray energies, the decrease in attenuation scales by roughly 5×2 per cent $= 10$ per cent. This is not sufficient to account for the marginal spectral hardening which appears in the intrinsically emitted VHE spectrum above ~300 GeV. The red symbols in Fig. [3](#) represent the intrinsic spectrum for the decreased attenuation estimated to result from a 2 per cent decrease in EBL density. The results of the calculations suggest that the *anisotropic* location of VHE-like sources with respect to intervening voids cannot be entirely accounted for by a lower EBL photon density inside a void as compared to outside a void.

An alternative explanation of the distribution of extragalactic VHE-like sources is dependent on the magnitude of the magnetic field within intervening voids. Proposed astrophysical mechanisms for generating large-scale magnetic fields predict little magnetic flux inside void regions (Beck et al. [2013](#)), while primordial generation mechanisms can create arbitrarily large void magnetic fields, though the latter mechanisms are somewhat constrained by cosmic microwave background (CMB) polarization observations (see Carilli & Taylor [2002](#) for a review). With a low intervening magnetic field within voids, the pair cascades resulting from EBL and VHE photon interaction and/or cosmic ray interaction would remain close to the direct LoS. The pairs will often have sufficient energy to upscatter CMB and EBL photons to gamma-ray energies, as described in Neronov & Vovk ([2010](#)). Observation of gamma-ray variability above and below the gamma-ray opacity of ~2 can be used to test the feasibility of secondary cascade emission contributing a significant portion of the observed gamma-ray flux.

In summary, this work shows preliminary but intriguing indications for a non-trivial relationship between the properties of VHE-like sources and the LoS void intersection. The investigation of the distribution of sources as related to the fraction of intervening underdense regions hints that VHE-like sources are located preferentially along underdense lines of sight. This same correlation does not appear for randomly distributed points, SDSS quasars or lower energy gamma-ray active galactic nuclei (AGN). Moreover, the percentage of sources that fall within voids are consistent across the randomly distributed, SDSS quasar, 2LAC, 1FHL and VHE-like populations. In other words, all source types are distributed in a similar fashion within the cosmic web, but only VHE-like sources are correlated on the sky with low-density lines of sight. Expanding this study to include more sources and voids will take years of observational effort but is likely necessary to determine if the marginal correlation found here is a statistical fluctuation. The results presented here, not accounted for by regions of lower EBL density, suggest that VHE detection of extragalactic sources may not solely depend on the intrinsic VHE emission from a source, but instead depends on a convolution of the source VHE emission and location within the cosmic web.

ACKNOWLEDGEMENTS

REFERENCES

Ackermann M. et al., 2011, ApJ, 743, 171
Ackermann M. et al., 2012, Science, 338, 1190
Ackermann M. et al., 2013, ApJS, 209, 34
Aharonian F. et al., 2006, Nature, 440, 1018
Archambault S. et al., 2014, ApJ, 785, L16
Atwood W. B. et al., 2009, ApJ, 697, 1071
Barnacka A., Böttcher M., Sushch I., 2014, ApJ, 790, 147
Becherini Y., Boisson C., Cerruti M. H.E.S.S. Collaboration 2012, in Aharonian F. A., Hofmann W., Riege F. M., eds, AIP Conf. Proc. Vol. 1505, High Energy Gamma-Ray Astronomy: 5th International Meeting on High Energy Gamma-Ray Astronomy. Am. Inst. Phys., New York, p. 490
Beck A. M., Hanasz M., Lesch H., Remus R. S., Stasyszyn F. A., 2013, MNRAS, 429, 60

Carilli C. L., Taylor G. B., 2002, ARA&A, 40, 319

Harris J., Chadwick P. M., 2014, J. Cosmol. Astropart. Phys., 10, 018

Coleman R., 1989, Can. J. Stat., 17, 27

Domínguez A. et al., 2011a, MNRAS, 410, 2556

Domínguez A., Sanchez-Conde M., Prada F., 2011b, J. Cosmol. Astropart. Phys., 11, 020

Domínguez A., Finke J. D., Prada F., Primack J. R., Kitaura F. S., Siana B., Paneque D., 2013, ApJ, 770, 77

Eisenstein D. J. et al., 2001, AJ, 122, 2267

Essey W., Kusenko A., 2010, Astropart. Phys., 33, 81

Franceschini A., Rodighiero G., Vaccari M., 2008, A&A, 487, 837

Furniss A. et al., 2013, ApJ, 768, L31

Gilmore R., Somerville R., Primack J., Dominguez A., 2012, MNRAS, 422, 3189

Gould R. J., Shréder G., 1967, Phys. Rev., 155, 1408

Hauser M., Dwek E., 2001, ARA&A, 39, 249

Horns D., Meyer M., 2012, J. Cosmol. Astropart. Phys., 2, 33

MAGIC Collaboration, 2008, Science, 320, 1752

Mattox J. et al., 1996, ApJ, 461, 396

Meyer M., Raue M., Mazin D., Horns D., 2012, A&A, 542, 59

Meyer M., Montanino D., Conrad J., 2014, J. Cosmol. Astropart. Phys., 09, 003

Neronov A., Vovk I., 2010, Science, 328, 73

Neyrinck M. C., 2008, MNRAS, 386, 2101

Nikishov A. I., 1962, Soviet Phys. JETP, 14, 393

Platen E., van de Wygaert R., Jones B., 2007, MNRAS, 380, 551

Rubtsov G. I., Troitscky S. V., 2014, preprint (arXiv:1406.0239)

Schneider D. P. et al., 2010, AJ, 139, 2360

Strauss M. A. et al., 2002, AJ, 124, 1810

Sutter P. M., Lavaux G., Wandelt B. D., Weinberg D. H., 2012, ApJ, 761, 44

Sutter P. M., Lavaux G., Wandelt B. D., Weinberg D. H., Warren M. S., 2013, MNRAS, 438, 3177

Sutter P. M. et al., 2015, A&C, 9, 1

Tavecchio F., Roncadelli M., Galanti G., 2014, preprint (arXiv:1406.2303)

This paper has been typeset from a TEX/LATEX file prepared by the author.